Bandgap Engineering of InGaAsP/InP Multiple Quantum Well Structure by Dielectric Sputtering

Hongli Zhu, Yuan Zhuang, Xin Zhang, and Jian-Jun He
Centre for Integrated Optoelectronics, State Key Laboratory of Modern Optical Instrumentation
Department of Optical Engineering, Zhejiang University, Hangzhou 310027, China

Abstract— This paper investigates a method of Si_3N_4 sputtering and annealing on quantum well intermixing for bandgap engineering of InGaAsP/InP multiple quantum well structure. A bandgap blueshift of about 90 nm is obtained. At the same time, the PL peak width becomes narrower, and the intensity is slightly increased. The waveguide losses at the absorption edge of the waveguide with and without QWI are about 27 dB/cm and 39 dB/cm, respectively. The results indicate the good quality of the MQW material after the bandgap engineering by dielectric sputtering and annealing.

1. INTRODUCTION

The InGaAsP/InP multiple quantum well (MQW) heterostructure is a widely used material system for 1.55 μm optical communication lasers. Recently, photonic integrated circuit (PIC) has attracted more and more attention for its high-functionality, low-cost, and low-power-consumption [1]. A key issue in the fabrication of PICs is the bandgap engineering of the MQW wafer in order to monolithically integrate active and passive devices. Quantum well intermixing (QWI) is a promising method that can selectively shift the bandgap post-growth with simple process [2]. In this paper, we present our recent work on QWI by dielectric sputtering method [3, 4].

2. EXPERIMENTS

The sample is a 1.2% compressive strained laser structure containing five $In_{0.8}Ga_{0.2}As_{0.8}P_{0.2}$ QWs with 1.25Q InGaAsP barriers, with the emission wavelength around 1.54 μm. From the surface, the layers are a 0.5 μm Zn-doped (10^{18} cm^{-3}) InP sacrificial layer, 0.2 μm Zn-doped (10^{19} cm^{-3}) $In_{0.53}Ga_{0.47}As$ cap, 1.5 μm Zn-doped (10^{18} cm^{-3}) InP upper cladding, 0.004 μm Zn-doped (4×10^{17} cm^{-3}) l.3Q InGaAsP etch-stop layer, five repeats of l0 nm undoped $In_{0.8}Ga_{0.2}As_{0.8}P_{0.2}$QW and 5.5 nm undoped InGaAsP QW which is sandwiched by two 0.06 μm InGaAsP step-graded index confining layers, and 1.5 μm Si-doped (2×10^{18} cm^{-3}) InP buffer on Si-doped (4×10^{18} cm^{-3}) InP substrate. All the layers are grown by MOCVD.

Samples with and without QWI processing were fabricated on a monolithic chip. To compare the difference between them, a patterned layer of photoresist of 1.6 μm thick was used to protect the no-QWI region. The sample was first pre-processed with argon plasma for a very short time. The plasma source used in the experiment is Oxford Plasmalab System 100. The ICP chamber was set to 20 sccm Ar flow rate and 4 mTorr pressure. The RF power and ICP power were 500 W both, with a DC bias of 741 V. After being exposed under Ar plasma in the ICP chamber for 10 seconds, a dielectric layer of Si_3N_4 was deposited by sputtering method. The deposition was carried out at a RF power of 200 W with DC bias of 482 V and a chamber pressure of 20 mTorr with a chamber temperature of 20°C. Then the photoresist was removed by acetone. After that, the sample was annealed at 750°C for 120 seconds in a flowing nitrogen atmosphere using a rapid thermal anneal (RTA). Silicon caps were used during the RTA process to prevent phosphorus out-diffusion. At last, the sample was wet etched by hydrochloric acid solution for 45 seconds to remove the Si_3N_4 by lift-off of sacrificial layer. Photoluminescence (PL) measurement was then carried out at room temperature to assess the bandgap shift.

To evaluate the influence of the QWI process, waveguide loss measurement by Fabry-Perot fringe technique was performed. Straight ridge waveguides were fabricated with 2.5 μm width and 1.6 μm height by the standard dry-etch technology. The sample was then cleaved to form a 900-μm-long Fabry-Perot cavity. A tunable laser (1.46–1.64 μm) was used as the input light source. The light was coupled into the waveguide through a polarization preserving lens fiber in TE mode. The output light was coupled by a lens fiber into an InGaAs detector.

3. RESULTS AND DISCUSSION

Figure 1 shows the measured PL map of the sample for peak wavelength (a), peak intensity (b), and full-width-at-half-maximum (FWHM) (c). A comparison table is given in (d). The peak wavelength is about 1536 nm for the protected region, and is blue shifted to 1446 nm for the QWI region. The intensity of the QWI region is increased by about 30% while the FWHM is reduced from 125 nm to 92 nm. The wavelength blue shift of about 90 nm shows the effectiveness of the QWI based on Si_3N_4 sputtering. The slightly enhanced peak intensity and narrowed FWHM indicate that this method has the ability to maintain or improve the property of the QWs.

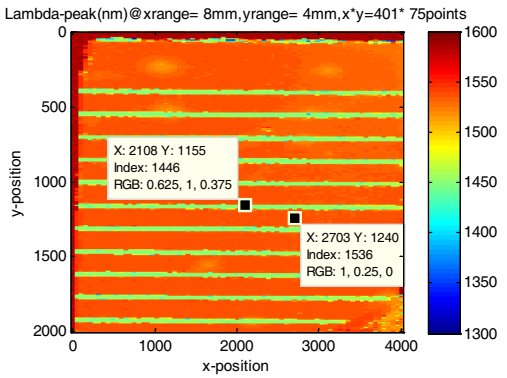

(a)

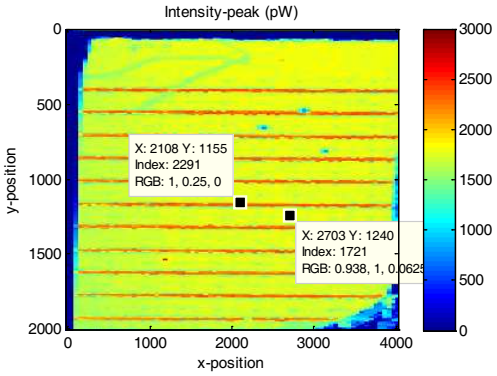

(b)

	with_QWI	without_QWI	difference
peak-wavelength(nm)	1446	1536	-90
peak-intensity(a.u.)	2291	1721	+33%
FWHM(nm)	92	125	-33

(c)

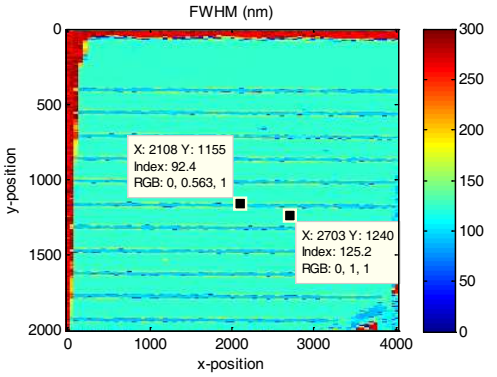

(d)

Figure 1: (a) Peak wavelength, (b) peak intensity, (c) FWHM of PL spectrum respectively for the same sample, and (d) the comparison table.

Figure 2 shows the measured transmission spectra of with and without QWI waveguides. {Red line refers to without QWI waveguide, and blue line refers to with QWI waveguide, respectively.} From the band edges of the two spectra, we can derive a net blue shift of about 85 nm with the QWI, which is consistent with the peak wavelength shift of the PL measurement in Figure 1(a). The Fabry-Perot interference fringe is generated due to the multiple reflectance of the two cleaved facets. Its contrast is related to the loss constant of the waveguide. We can therefore derive the loss coefficients of the waveguides as a function of the wavelength. It should be noted that, for wavelength shorter than the bandgap, the Fabry-Perot fringes disappear due to high absorption, and therefore another method based on the relative transmission intensity is used [5–7].

Figure 3 compares the loss coefficients derived from the measured transmission spectra for the waveguides with and without QWI. For wavelength slightly longer than the absorption edge, the measured loss is about 27 dB/cm at 1635 nm for the sample without QWI, while it is reduced to 20 dB/cm at 1550 nm for the sample with QWI. The loss further decreases to 18 dB/cm at 1635 nm for the intermixed waveguide. It should be noted that the loss in the QWI waveguide appears to be lower than that of the sample without QWI, even after considering the 85 nm difference in bandgaps. This indicates that no excess loss results from the QWI process, which is consistent with the slightly increased peak intensity of the PL measurement in Figure 1(b).

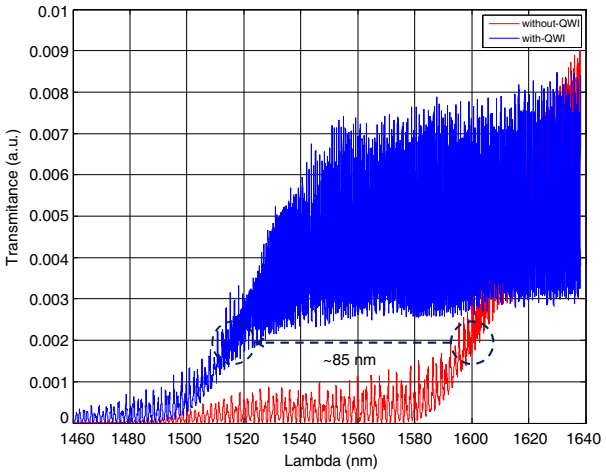

Figure 2: Measured transmission spectra of waveguides with and without QWI.

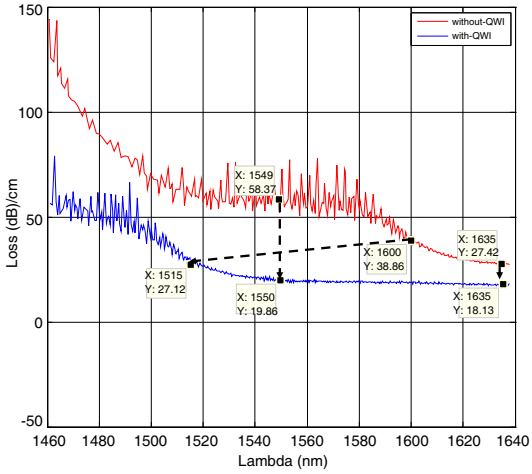

Figure 3: Loss coefficients derived from the measured transmission spectra of waveguides with and without QWI.

4. CONCLUSION

We have reported the experimental results on QWI experiment using Si_3N_4 sputtering and annealing. A maximum blue-shift of 90 nm has been achieved with a PL intensity enhancement and linewidth reduction. The waveguide loss measurement shows a reduced loss after the QWI process from 27 dB/cm to 18 dB/cm in the transparent region near the absorption edge. The technique is therefore suitable for active-passive integration in PIC applications.

ACKNOWLEDGMENT

This work was supported by the National High-Tech R&D Program of China (grant No. 2011AA010305), and the National Natural Science Foundation of China (grant No. 61377038).

REFERENCES

1. Raring, J. W. and L. A. Coldren, "40 Gbps widely tunable transceivers," *IEEE J. Sel. Topics Quantum Electron.*, Vol. 13, No. 1, 3–14, 2007.
2. Parker, J. S., J. S. Parker, A. Sivananthan, E. Norberg, and L. A. Coldren, "Regrowth-free high-gain InGaAsP-InP active-passive platform via ion implantation," *Optics Express*, Vol. 20, No. 18, 19947–19955, 2012.
3. Kowalski, O. P., C. J. Hamilton, S. D. McDougall, J. H. Marsh, A. C. Bryce, R. M. De La Rue, B. Vogele, and C. R. Stanley, "A universal damage induced technique for quantum well intermixing," *Applied Physics Letters*, Vol. 72, No. 5, 581–583, 1998.
4. McDougall, S. D., O. P. Kowalski, C. J. Hamilton, F. Camacho, B. Qiu, M. Ke, R. M. De La Rue, A. C. Bryce, and J. H. Marsh, "Monolithic integration via a universal damage enhanced quantum well intermixing technique," *IEEE J. Sel. Topics Quantum Electron.*, Vol. 4, No. 4, 636–646, 1998.
5. He, J. J., Y. Feng, E. S. Koteles, J. P. Poole, M. Davis, M. Dion, R. Goldberg, I. Mitchell, and S. Charbonneau, "Bandgap shifted InGaAsP/InP quantum well waveguides using MeV ion implantation," *Electronics Letters*, Vol. 31, No. 24, 2094–2095, 1995.
6. Charbonneau, S., E. S. Koteles, P. J. Poole, J. J. He, G. C. Aers, J. Haysom, M. Buchanan, Y. Feng, A. Delage, F. Yang, M. Davies, R. D. Goldberg, P. G. Piva, and I. V. Mitchell, "Photonic integrated circuits fabricated using ion implantation," *IEEE J. Sel. Topics Quantum Electron.*, Vol. 4, No. 4, 772–793, 1998.
7. Zhang, X. and J. J. He, "Optical loss of bandgap shifted lnGaAsP/lnP waveguide using argon plasma-enhanced quantum well intermixing," *Advances in Optoelectronics and Micro/Nano-Optics*, 2010.